

Original article

DOI: <https://doi.org/10.18721/JPM.14408>

STRUCTURE CHARACTERISTICS OF NANOPOROUS GLASS WITH THE CARBON-MODIFIED INTERFACE

*S. A. Udovenko*¹ , *A. A. Naberezhnov*², *S. A. Borisov*²,
*A. A. Sysoeva*², *M. V. Tomkovich*², *A. Kh. Islamov*³, *A. I. Kuklin*³

¹ Peter the Great St. Petersburg Polytechnic University, St. Petersburg, Russian Federation

² Ioffe Institute, St. Petersburg, Russia

³ Frank Laboratory of Neutron Physics, Joint Institute for Nuclear Research, Dubna, Russia

 udovenko_sa@spbstu.ru

Abstract: Samples of porous matrices with the surface of channels (pores) modified with carbon were prepared on the basis of nanoporous sodium borosilicate glasses (SBS) with average pore diameter of 6 ± 0.5 (PG6) nm. A procedure has been developed for introduction of carbon into the PG6 channels from an aqueous solution of sucrose with its subsequent thermal decomposition. X-ray diffraction studies of the state of carbon in the pores of the obtained modified matrix have been carried out. The small-angle neutron scattering method is used for study of internal spatial arrangement of these matrices and to obtain information concerning to the state of channel surfaces in these samples. A combined analysis of the data obtained by X-ray diffraction and from the results of small-angle neutron scattering have shown that the process of thermal decomposition of sucrose in the channels leads to the formation of amorphous carbo layers on the internal surface of the channels (pores) in these glasses, i.e. the «matrix-porous space» interface is being modified.

Keywords: nanoporous borosilicate glasses, modification of interface, small angle neutron scattering, X-ray diffraction.

Citation: Udovenko S. A., Naberezhnov A. A., Borisov S. A., Sysoeva A. A., Tomkovich M. V., Islamov A. Kh., Kuklin A. I., Structure characteristics of nanoporous glass with the carbon-modified interface, St. Petersburg Polytechnical State University Journal. Physics and Mathematics. 14 (3) (2021) 114–125. DOI: 10.18721/JPM.14408

This is an open access article under the CC BY-NC 4.0 license (<https://creativecommons.org/licenses/by-nc/4.0/>)



Научная статья

УДК 538.971, 539.26

DOI: <https://doi.org/10.18721/JPM.14408>

СТРУКТУРНЫЕ ХАРАКТЕРИСТИКИ НАНОПОРИСТОГО СТЕКЛА С ИНТЕРФЕЙСОМ, МОДИФИЦИРОВАННЫМ УГЛЕРОДОМ

С. А. Удовенко¹ ✉, А. А. Набережнов², С. А. Борисов²,
А. А. Сысоева², М. В. Томкович², А. Х. Исламов³, А. И. Куклин³

¹ Санкт-Петербургский политехнический университет Петра Великого, Санкт-Петербург, Россия;

² Физико-технический институт им. А.Ф. Иоффе РАН, Санкт-Петербург, Россия;

³ Лаборатория нейтронной физики им. И. М. Франка Объединенного института ядерных исследований, г. Дубна, Россия

✉ udovenko_sa@spbstu.ru

Аннотация. С целью создания нанокompозитных материалов на основе искусственных нанопористых матриц с модифицированным интерфейсом разработана процедура введения углерода С в каналы нанопористого натриево-боросиликатного стекла (РG6) со средним диаметром пор $6,0 \pm 0,5$ нм из водного раствора сахарозы с последующим ее термическим разложением. Образцы созданного материала РG6+С были исследованы методами адсорбционной порометрии азота (NAP), дифракции рентгеновского излучения (XRD) и малоуглового рассеяния нейтронов (SANS). В результате XRD-исследования были получены данные о состоянии углерода в порах (размер пор определяли методом NAP) созданной модифицированной матрицы, а метод SANS позволил выявить особенности внутреннего пространственного устройства данной матрицы и получить информацию о состоянии поверхности каналов в этих образцах. Совокупный анализ полученных результатов показал, что процесс термического разложения сахарозы в каналах приводит к формированию слоя аморфного углерода на внутренней поверхности каналов (пор) данного стекла, т. е. происходит модификация интерфейса «матрица – пора».

Ключевые слова: нанопористое боросиликатное стекло, модификация интерфейса, малоугловое рассеяние нейтронов, рентгеновская дифракция

Финансирование: В СПбПУ работы проводились при частичной финансовой поддержке Российского фонда фундаментальных исследований (RFBR-BRICS грант № 19-52-80019).

Для цитирования: Удовенко С. А., Набережнов А. А., Борисов С. А., Сысоева А. А., Томкович М. В., Исламов А. Х., Куклин А. И. Структурные характеристики нанопористого стекла с интерфейсом, модифицированным углеродом // Научно-технические ведомости СПбГПУ. Физико-математические науки. 2021. Т. 4 № .14. С. 125–114. DOI: 10.18721/JPM.14408

Статья открытого доступа, распространяемая по лицензии CC BY-NC 4.0 (<https://creativecommons.org/licenses/by-nc/4.0/>)

Introduction

The link between confined geometry, in particular, the size effect, and the macroscopic physical properties of materials is the focus of much attention, as it is one of the most pressing problems in modern condensed matter physics, with experiments and theoretical models confirming that these properties are considerably modified in this case. The primary interest lies in the nanocomposite materials (NCM) based on natural and artificial nanoporous frameworks, which are actively used as porous glasses, opals, chrysotile asbestos, MCM-41 (48) and SBA-15 molecular sieves, etc. The existing methods for NCM synthesis allow obtaining materials with magnetics, ferroelectrics, semiconductors, metals, liquids and other substances embedded in the pore space. Modern experimental equipment can be used to study the relationship of the size effect and confined geometry with the crystal structure, phase transitions (PT), transport properties and other characteristics of nanostructured substances.

Notably, tailoring the type of framework and the mean diameter of the channels makes it possible to trace the correlation between the size of a nanoparticle (and sometimes its shape) and the properties, assessing the role that the framework itself (in particular, the interface between the framework and the embedded material) and its topology (spatial arrangement) play in inducing new macroscopic physical properties in nanocomposite materials.

Unfortunately, the effect of the interface on the properties of NCM has been poorly understood; for this reason, the goal of this study consisted of producing a new type of porous frameworks based on porous glasses (PG) with the mean pore diameter of 6 nm (PG6), where the interface between the framework and the pore space is modified by carbon coating.

The majority of PG-based NCM considered previously were prepared by embedding materials into pores either from an aqueous solution or from a melt. Coating the surface of nanochannels with carbon dramatically alters the wettability of the framework by the embedded aqueous solution/melt, potentially leading to major transformation in the spatial arrangement of nanoparticles in these nanocomposites, and therefore in the physical characteristics (macroscopic properties) of NCM. Our plan was not only to fabricate frameworks with a modified interface but also to compare their characteristics with similar parameters of pure PG6 glasses, obtaining data on the state of carbon coating in novel porous glasses. Nitrogen adsorption porometry (NAP), X-ray diffraction (XRD) and small-angle neutron scattering (SANS) were used to examine the properties of the frameworks.

Sample preparation and experimental methods

Porous sodium borosilicate (SBS) glasses with a mean pore diameter of 6.0 ± 0.5 nm (PG6) were used to prepare glasses with a carbon-modified interface; these are the so-called microporous glasses, obtained after partially removing the chemically unstable phase appearing during phase separation [1]. The pore diameter in the original PG6 frameworks was determined by mercury porosimetry; pores in these glasses comprise a random open 3D network of interconnected channels, that is, a dendritic structure.

Porous glasses were prepared by the standard procedure [1] at the Ioffe Institute. Fig. 1 schematically shows the spatial arrangement of an 'empty' PG6 glass. The pore space in the channels between the secondary silica particles (mainly consisting of silicon dioxide SiO_2 and formed after acid etching of pure glasses) and the framework consisting of amorphous SiO_2 is precisely what generates a random 3D network of interconnected nanochannels with a mean diameter of about 6 nm in this glass.

The samples for the measurements were rectangular plates of microporous SBS with the dimensions not exceeding $10.0 \times 4.0 \times 0.5$ mm (due to the requirements imposed on the samples for SANS measurements with the setup). The porosity of these glasses was approximately 23% of the total sample volume. The sample of pure PG6 glass taken for SANS measurements weighed 21.1 mg; the sample of pure PG6 glass taken for carbon filling was 30.3 mg; the carbon embedded into this sample weighed 1.6 mg (about 5%).

The glass plates prepared were processed as follows. First, pure porous glass was annealed in air for a day at a temperature of 500 °C. Then the glass was immersed in a 15% aqueous sucrose solution (GR grade) and slowly heated to 200 °C. As sucrose started to decompose,

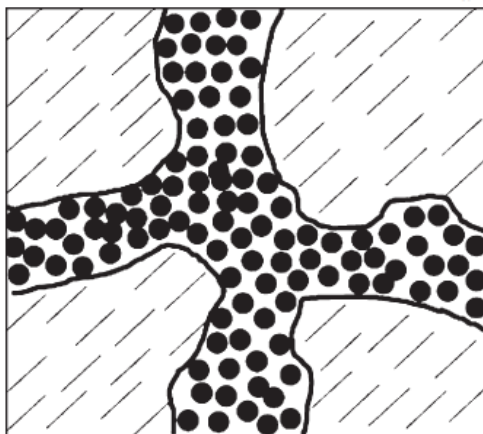


Fig. 1. Schematic spatial arrangement of the microstructure in microporous alkali borosilicate glasses [1]:

framework joints (shaded) consist mainly of SiO_2 ; a microporous structure evolves in the region of the chemically unstable phase (CUP, the remaining space) after the first cycle of acid etching; secondary silica (black circles) has its own internal structure; the surfaces of the channels where CUP emerges are shown by black lines

the temperature was slowly raised to $300\text{ }^\circ\text{C}$, and the sample was held at this temperature for about 24 h. The temperature was increased to $350\text{ }^\circ\text{C}$ for 30 min at the final stage of annealing. The degree of pore saturation was determined by the gravimetric method; it amounted to approximately $16.5 \pm 2.3\%$ of the initial pore volume. Naturally, filling the pores with carbon was expected to produce a decrease in the total pore volume and specific surface area of the channels, so we measured the decrease in this area by adsorption porosimetry (the BET method, proposed by Brunauer, Emmett and Teller [2, 3]). The specific surface area was $68.27 \pm 0.14\text{ m}^2/\text{g}$ for pure PG6, and $49.58 \pm 0.48\text{ m}^2/\text{g}$ for glass with carbon, i.e., filling with carbon did in fact lead to a decrease in the specific surface area, while the overall change in this parameter was about 27%, which is in good agreement with the change in the pore volume.

Diffraction studies were conducted at room temperature with the SuperNova X-ray diffractometer system from Agilent Technologies (at Peter the Great St. Petersburg Polytechnic University) at 0.7092 E wavelength ($K_{\alpha 1}\text{Mo}$), in transmission mode; the incident beam was focused into a narrow spot on the sample surface.

The internal spatial arrangement in pure PG6 glasses and carbon-filled PG6 samples (referred to as PG6+C from now on) was analyzed using the YuMO spectrometer for small-angle neutron scattering [4–6] at the IBR-2 pulsed reactor (Frank Laboratory of Neutron Physics, Joint Institute for Nuclear Research, Dubna, Moscow Oblast, Russia).

The YuMO setup comprises two moving detector systems, with sample-to-detector distances of 5.28 and 13.4 m, covering the momentum transfer range of $0.006\text{--}0.500\text{ E}^{-1}$; the momentum transfer Q is defined as follows:

$$Q = (4\pi/\lambda) \cdot \sin(\theta/2),$$

where λ , E, is the neutron beam wavelength; θ is the scattering angle.

The beam can be collimated to a diameter of 14 mm, i.e., the samples were completely covered by the incident beam in our case. The obtained neutron scattering spectra were corrected for transmission and thickness of the samples, background scattering by the holders used (thin adhesive tape served as the holder in our case) and by a reference vanadium sample in the SAS package [7, 8]. The $I(Q)$ dependences were obtained as a result, corresponding to the neutron scattering intensity I versus the momentum transfer Q (cm^{-1} in absolute units).

Results and discussion

As a first stage of the study, we used X-ray diffraction to examine the state of carbon embedded into the pores of the PG6 glass. Fig. 2 shows the diffraction patterns for both pure and carbon-filled PG6 glasses. No pronounced diffraction peaks were observed in both cases, as evident from comparing the simulated spectrum of graphite (Fig. 2, vertical lines) expected for the given wavelength with the experimental spectrum for PG6+C (also shown in Fig. 2).

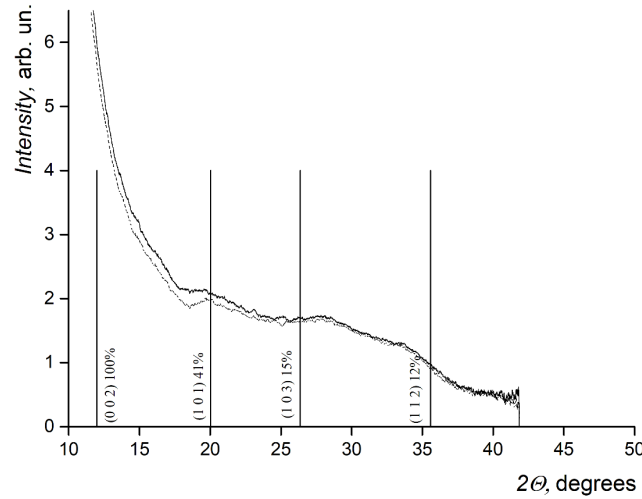


Fig. 2. XRD patterns for pure (dashed line) and carbon-filled (solid line) samples of porous PG6 glasses.

The vertical lines mark the positions of the most intense peaks in graphite (C) at a given wavelength (0.7092 E); the figure shows the intensity percentage for each reflection relative to the (002) peak

We believe that any other crystalline phases of carbon are unlikely to appear, considering the technique used for filling the pores (see above). It has been established that SiO_2 is in an amorphous state in a pure PG6 sample (the same can be concluded from analyzing the data in Fig. 2). Apparently, the spectra follow the same trend for both types of glasses; therefore, we can safely assume from the above that carbon is in an amorphous state in the PG6+C glass as well.

Notice the relative position of the curves: the one corresponding to scattering by PG6+C lies above that for PG6. Since the sample area illuminated by X-rays is the same in both cases (as follows from the geometry of the experiment), the samples have the same thickness and the same exposure time, additional scattering is associated with additional scattering centers, that is, carbon atoms, which is generally confirmed by our calculations.

Because our studies were aimed at exploring the internal structure in PG6+C glasses and comparing it with similar parameters for PG6 samples, we subsequently applied the SANS method, whose exact benefit is that it can provide data on the spatial arrangement in the given objects, including the size of particles in glasses and their fractal characteristics. The following relation is known for the intensity $I(Q)$ of neutron scattering by porous systems, [9]:

$$I(Q) \sim V_p^2 n_p^2 (\rho_p - \rho_s)^2 P(Q) S(Q), \quad (1)$$

where V_p , cm^3 , is the volume of the pores; n_p , cm^{-3} , is their spatial density; ρ_p and ρ_s , cm^{-2} , are the scattering-length densities of the material in the pores and in the framework, respectively; $P(Q)$ is the shape factor for pores (or particles in the framework); $S(Q)$ is the structure factor depending on spatial ordering of the pores (it describes the interference effects from the scattering controlled by the contrast between the pore and the framework); recall that Q , E^{-1} , is the momentum transfer (see above).

Considering disordered systems such as porous glasses, provided that there is no strong correlation between inhomogeneities (or fluctuations in the scattering length density) and given large Q values, the structure factor $S(Q)$ and the difference in the scattering-length density $(\Delta\rho)^2 = (\rho_p - \rho_s)^2$ play a major role in Eq. (1). Large values of Q are assumed to be those falling within the Porod region [10], where the condition $QR_g \geq 1$ is satisfied (R_g is the radius of gyration, or the root-mean-square radius of inertia for a scattering particle or pore).

In view of the above conditions, relation (1) is further simplified:

$$I(Q) = A \cdot Q^{-\alpha} + B, \quad (2)$$

where A , B are constants, and B is the background value at large Q .

It was found in [11] that the values of the exponent α for highly branched surfaces (surface fractals with the dimension D_s within $2 < D_s < 3$) lie in the interval $3 < \alpha \leq 4$, and the following expression holds true for the scattering intensity:

$$I(Q) = A \cdot Q^{-(6-D_s)} + B, \quad (3)$$

while the parameter $(\Delta\rho)^2$ is implicitly included in the constant A [11], that is, the quantity $\Delta\rho$ (often called the contrast) plays a fundamental role in the dependence of intensity I of small-angle neutron scattering on the momentum transfer Q .

Now let us consider the experimentally obtained dependences $I(Q)$ for PG6 and PG6+C glasses (Fig. 3). Notice that all data shown in Figs. 3 and 4 are normalized to the mass of the samples.

The fundamental difference between the glasses is that there is only a single interface separating the framework from the pore space in pure PG6 glass, which is what actually controls the scattering. Since the pore space is filled with air, we can assume that $\rho_p = 0$, so that the relation for total scattering is determined by the quantity ρ_s , written as follows for SiO_2 :

$$\rho_s = (b_{\text{Si}} + 2b_{\text{O}}) \cdot N_A \cdot d_s / M_{\text{mol}}, \quad (4)$$

where b_{Si} , b_{O} , cm, are the amplitudes of neutron scattering by silicon and oxygen nuclei, respectively, $b_{\text{Si}} = 4.149 \cdot 10^{-12}$ cm, $b_{\text{O}} = 5.803 \cdot 10^{-12}$ cm [12]; N_A , mol^{-1} , is the Avogadro number; d_s , g/cm^3 , is the physical density of glass, $d_s = 2.12$ g/cm^3 ; M_{mol} , g/mol , is the molar mass of SiO_2 , $M_{\text{mol}} = 60.084$ g/mol .

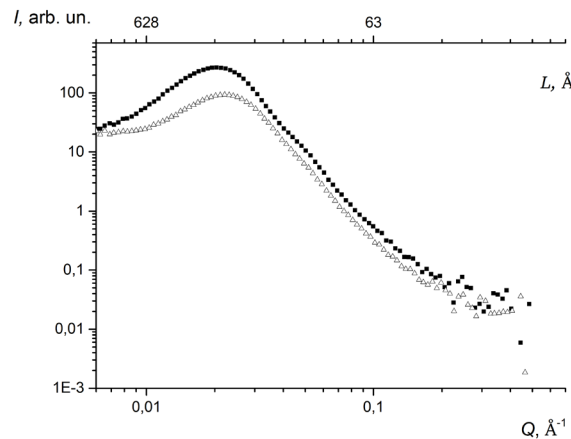


Fig. 3. Intensity of small-angle neutron scattering as a function of momentum transfer for pure PG6 (triangles) and carbon-filled PG6+C (squares) porous glasses.

The upper grid corresponds to the spatial scale L (Å) in direct space

Substituting the values, we obtain ρ_s :

$$\rho_s(\text{SiO}_2) = 3.35 \cdot 10^{10} \text{ cm}^{-2}.$$

There are three interfaces in the PG6+C glass sample: carbon/framework, carbon/pore space, and framework/pore space. Similar calculations by Eq. (4) for the scattering-length density of neutrons from carbon (in our case, $d_C = 2.15 \text{ g/cm}^3$, $b_C = 6.64 \cdot 10^{-12} \text{ cm}$ for graphite) yield $\rho_s(\text{C}) = 7.18 \cdot 10^{10} \text{ cm}^{-2}$. The scattering intensity is proportional to $(\Delta\rho)^2$; the values of $(\Delta\rho)^2$ are fairly large in the case of PG6+C at all three interfaces, so that the value for the interface between carbon and framework,

$$\Delta\rho = (7.18 - 3.35) \cdot 10^{10} = 3.83 \cdot 10^{10} \text{ cm}^{-2},$$

is higher than that for the interface between the framework and the pore space. A sharp increase in scattering by the PG6+C sample should be expected then, compared with PG6, which is observed in the experiment (see Fig. 3). On the other hand, as noted above, the relative fraction of carbon amounts to only about 5%, while the scattering (as evident from Fig. 3) increases by several times and even by an order of magnitude in the range $Q \approx 0.02 \text{ E}^{-1}$. It is self-evident that such an effect is possible only for well-developed interfaces produced through modification with carbon. The $I(Q)$ dependences also exhibit intensity peaks at $Q_{\text{max1}} \approx 0.0222 \text{ E}^{-1}$ for PG6 and at $Q_{\text{max2}} \approx 0.0203 \text{ E}^{-1}$ for PG6+C. As is well known, a modulated structure (correlation peak) forms in standard porous Vycor-type SBS glasses. This structure has a characteristic spatial scale $L \sim 2\pi/Q_{\text{max}}$, where L amounts to about 30–45 nm, and the scale does not depend on the mean pore diameter, exclusively characterizing porous matrices of this type. Filling a part of the pore space with carbon leads to a small (but clearly visible) shift in the position of the Q_{max2} peak towards a larger L (about 31 nm) compared with the corresponding value for PG6 (about 28 nm), while the peak itself becomes much more pronounced compared with the curve for PG6. The likely reason for this is that a new, additional spatial scale appears, related to regions with local ordering of carbon atoms.

The next stage of the study involved detailed analysis of the slopes in the $I(Q)$ dependences for PG6 and PG6+C samples in the region with large momentum transfer Q , where the Porod law would be expected to be fulfilled (Fig. 4); according to this law, $I(Q) \sim Q^{-4}$. Indeed, the law is apparently well satisfied for both samples in the range of Q values from 0.03 to 0.10 E^{-1} , suggesting scattering by the smooth surface of channels (pores). If $Q \approx 0.1 \text{ E}^{-1}$ (this corresponds to a spatial scale of about 6 nm, i.e., the mean channel diameter according to mercury porosimetry data given earlier), crossover is observed in the behavior of the $I(Q)$ dependences. A region where

Table

Nitrogen adsorption porosimetry data for glass samples considered

Glass sample	Mean pore diameter, nm	
	for adsorption	for desorption
PG 6	12.70	7.03
PG 6+C	8.31	4.73

Notations: PG6 and PG 6+C correspond to pure porous SBS glass with a mean pore diameter of 6 nm and the same glass filled with carbon (C).

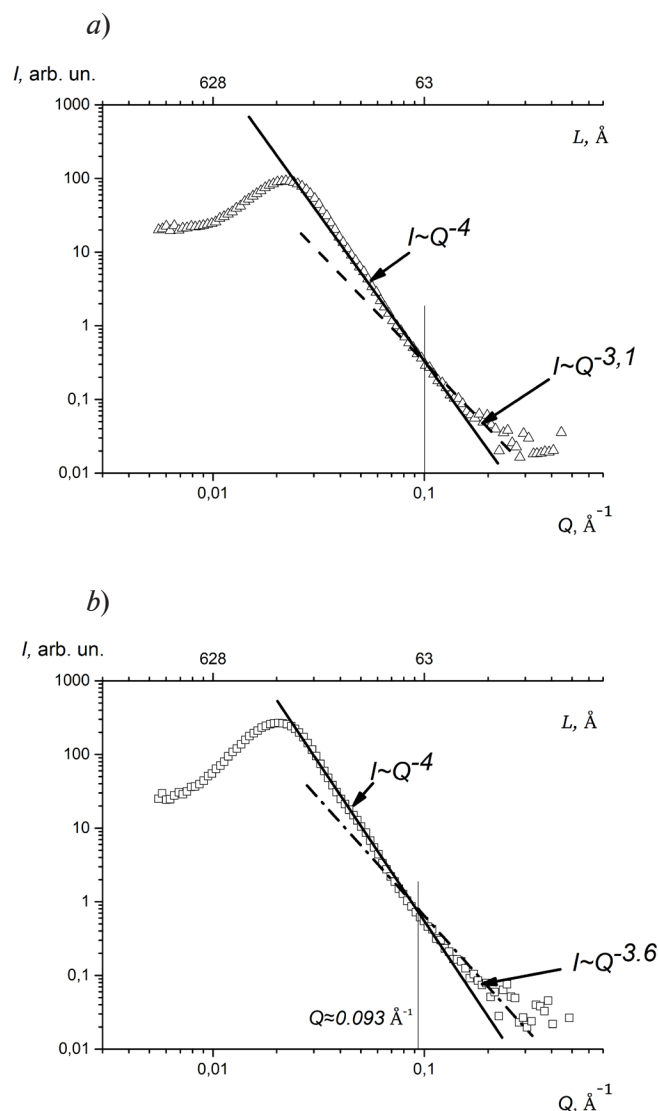


Fig. 4. Detailed analysis of the dependences for PG6 (a) and PG6+C (b) samples shown in Fig. 3, in the region where the Porod law $I(Q) \sim Q^{-4}$ is fulfilled (marked by straight solid lines).

The upper grids correspond to the spatial scale L (E) in direct space

$I(Q) \sim Q^{-3.1}$ (dashed line in Fig. 4, a) can be reliably detected for pure PG6 in the range $0.100 < Q < 0.178 \text{ E}^{-1}$, corresponding to scattering by a surface with a well-developed fractal structure. This is either scattering by the elements of the internal structure in secondary silica particles (see Fig. 1), or by the elements of the spatial structure of the entire chemically unstable phase. Filling the porous PG6 glass with carbon leads to a sharp increase in the parameter α up to 3.6 (see Fig. 4, b), that is, spatial branching is partially removed from the CUP surface and the value of this parameter approaches 4, characteristic for Porod's law ($\alpha \approx 4$). If this is the case, a decrease in the mean pore diameter should be observed as a result. We verified this assumption using nitrogen adsorption porosimetry and obtained the results presented in Table.

The data presented are clear evidence that filling the PG6 glass with carbon considerably modifies the spatial arrangement of the pore space of the resulting new framework, i.e., carbon not only covers the surface of the channels where CUP evolves (see Fig. 1), but also the CUP particles themselves; the mean diameter of the channels between these particles also partially decreases.

Conclusion

Analyzing the XRD and SANS spectra, we have established that embedding carbon into the pore space of pure porous SBS glass with a mean pore diameter of 6 nm (PG6) modifies the internal structure of the pore space. We have confirmed that the carbon embedded into the pores (channels) of the initial framework is in an amorphous state, producing layers in this space both on the surface of the channels, where a chemically unstable phase (CUP) evolves, and on the CUP particles. A sharp increase in the scattering intensity $I(Q)$ in the PG6+C sample compared with PG6 (despite the small mass fraction of carbon embedded into the pores) suggests that well-developed interfaces carbon-filled emerge. The intensity of small-angle scattering in the region of high momentum transfer Q is in good agreement with Porod's law, i.e., scattering by channels with a smooth surface.

Thus, we have obtained nanoporous frameworks with carbon-modified interfaces.

These frameworks were used to synthesize new nanocomposite materials (NCM); as the next stage of research, we plan to embed ferroelectrics (whose properties were previously studied only for standard nanoporous SBS) into the pores of these NCM to gain data on the effect of the modified interface on the macroscopic physical properties of NCM.

REFERENCES

1. Mazurin O. V., Roskova G. P., Averyanov V. I., Antropova T. V., Dvukhfaznyye stekla. Struktura, svoystva, primeneniye [Two-phase glasses: structure, properties and applications], Ed. by B. G. Varshal, Nauka, Leningrad, 1991 (in Russian).
2. Lowell S., Shields J., Thomas M. A., Thommes M., Characterization of porous solids and powders: surface area, porosity, and density (Particle Technology Series, Vol. 16). Springer Netherlands, Amsterdam, Berlin, 2004.
3. Barrett E. P., Joyner L. G., Halenda P. P., The determination of pore volume and area distributions in porous substances. I. Computations from nitrogen isotherms, *J. Am. Chem. Soc.* 73 (1) (1951) 373–380.
4. Ostanevich Yu. M., Time-of-flight small angle scattering spectrometers on pulsed neutron sources, *Makromol. Chem. Macromol. Symp.* 15(1) (1988) 91–103.
5. Kuklin A. I., Islamov A. Kh., Gordeliy V. I., Two-detector system for small-angle neutron scattering instrument, *Neutron News.* 16 (3) (2005) 16–18.
6. Kuklin A. I., Soloviev D. V., Rogachev A. V., et al., New opportunities by modernized small-angle neutron scattering two-detector system instrument (YuMO), *J. Phys.: Conf. Ser.* 291 (1) (2011) 012013.
7. Soloviev A. G., Solovieva T. M., Stadnik A. V., et al., SAS, The package for small-angle neutron scattering data treatment, Version 2.4, Long Write-Up and User's Guide, JINR Communication, Dubna, 2003, 086 (P10-2003-86) (2.337.706).
8. Soloviev A. G., Solovieva T. M., Ivankov O. I., et al., SAS program for two-detector system: seamless curve from both detectors, *J. Phys. Conf. Ser.* 848 (2017) 012020.
9. Ramsay J. D. F. Surface and pore structure characterization by neutron scattering techniques, *Adv. Colloid Interface Sci.* 76–77 (1 July) (1998) 13–37.
10. Teixeira J., Small-angle scattering by fractal systems, *J. Appl. Crystallogr.* 21 (6) (1988) 781–785.
11. Bale H. D., Schmidt P. W., Small-angle X-ray-scattering investigation of submicroscopic porosity with fractal properties, *Phys. Rev. Lett.* 53 (6) (1984) 596–599.
12. Neutron diffraction commission, Coherent neutron scattering amplitudes, *Acta Crystallogr. Section A.* 25 (2) 391–392.
13. Höhr A., Neumann H.-B., Schmidt P. W., et al., Fractal surface and cluster structure of controlled-pore glasses and Vycor porous glass as revealed by small-angle X-ray and neutron scattering, *Phys. Rev. B.* 38 (2) (1988) 1462–1467.
14. Levitz P., Ehret G., Sinha S. K., Drake G. M., Porous Vycor glass: The microstructure as probed by electron microscopy, direct energy transfer, small-angle scattering, and molecular adsorption, *J. Chem. Phys.* 95 (8) (1991) 6151–6161.



СПИСОК ЛИТЕРАТУРЫ

1. Мазурин О. В., Роскова Г. П., Аверьянов В. И., Антропова Т. В. Двухфазные стекла. Структура, свойства, применение. Под ред. Б. Г. Варшал. Ленинград: Наука, 1991. 276 с.
2. Lowell S., Shields J., Thomas M. A., Thommes M. Characterization of porous solids and powders: surface area, porosity, and density (Particle Technology Series. Vol. 16). Amsterdam, Berlin: Springer Netherlands, 2004. 350 p.
3. Barrett E. P., Joyner L. G., Halenda P. P. The determination of pore volume and area distributions in porous substances. I. Computations from nitrogen isotherms // Journal of the American Chemical Society. 1951. Vol. 73. No. 1. Pp. 373–380.
4. Ostanevich Yu. M. Time-of-flight small angle scattering spectrometers on pulsed neutron sources // Makromolekulare Chemie. Macromolecular Symposia. 1988. Vol. 15. No. 1. Pp. 91–103.
5. Kuklin A. I., Islamov A. Kh., Gordeliy V. I. Two-detector system for small-angle neutron scattering instrument // Neutron News. 2005. Vol. 16. No. 3. Pp. 16–18.
6. Kuklin A. I., Soloviov D. V., Rogachev A. V., et al., New opportunities by modernized small-angle neutron scattering two-detector system instrument (YuMO) // Journal of Physics: Conference Series. 2011. Vol. 291. No. 1. P. 012013
7. Соловьев А. Г., Соловьева Т. М., Стадник А. В., Исламов А. Х., Куклин А. И. SAS-программа для первичной обработки спектров малоуглового рассеяния. Версия 2.4. Описание и руководство пользователя // Сообщения Объединенного института ядерных исследований. Дубна. 2003. 086 (P10-2003-86) (2.337.706).
8. Soloviev A. G., Solovieva T. M., Ivankov O. I., Soloviov D. V., Rogachev A. V., Kuklin A. I. SAS program for two-detector system: seamless curve from both detectors // Journal of Physics: Conference Series. 2017. Vol. 848. P. 012020.
9. Ramsay J. D. F. Surface and pore structure characterization by neutron scattering techniques // Advances in Colloid and Interface Science. 1998. Vol. 76–77. 1 July. Pp. 13–37.
10. Teixeira J. Small-angle scattering by fractal systems // Journal of Applied Crystallography. 1988. Vol. 21. Part 6. December. Pp. 781–785.
11. Bale H. D., Schmidt P. W. Small-angle X-ray-scattering investigation of submicroscopic porosity with fractal properties // Physical Review Letters. 1984. Vol. 53. No. 6. Pp. 596–599.
12. Neutron diffraction commission. Coherent neutron scattering amplitudes // Acta Crystallographica. Section A. 1969. Vol. 25. Part 2. 1 March. Pp. 391–392.
13. Höhr A., Neumann H.-B., Schmidt P. W., Pfeifer P., Avnir D. Fractal surface and cluster structure of controlled-pore glasses and Vycor porous glass as revealed by small-angle X-ray and neutron scattering // Physical Review B. 1988. Vol. 38. No. 2. Pp. 1462–1467.
14. Levitz P., Ehret G., Sinha S. K., Drake G. M. Porous Vycor glass: The microstructure as probed by electron microscopy, direct energy transfer, small-angle scattering, and molecular adsorption // The Journal of Chemical Physics. 1991. Vol. 95. No. 8. Pp. 6151–6161.

THE AUTHORS

UDOVENKO Stanislav A.

Peter the Great St. Petersburg Polytechnic University
29 Politechnicheskaya St., St. Petersburg, 195251, Russia
udovenko_sa@spbstu.ru
ORCID: 0000-0002-0364-0797

NABEREZHNOV Aleksandr A.

Ioffe Institute of RAS
26 Polytekhnicheskaya St., St. Petersburg, 194021, Russia
alex.nabereznov@mail.ioffe.ru
ORCID: 0000-0003-1929-032X

BORISOV Sergey A.

Ioffe Institute of RAS

26 Politekhnikeskaya, St Petersburg 194021, Russia

sergey.borisov@mail.ioffe.ru

ORCID: 0000-0002-7486-0391

SYSOIEVA Anna A.

Ioffe Institute of RAS

26 Polytekhnikeskaya St., St. Petersburg, 194021, Russia

annasysoeva07@mail.ru

ORCID: 0000-0002-8876-9185

TOMKOVICH Maria V.

Ioffe Institute of RAS

26 Polytekhnikeskaya St., St. Petersburg, 194021, Russia

marya.tom83@gmail.com

ORCID: 0000-0002-1537-4107

ISLAMOV Akhmed Kh.

Joint Institute for Nuclear Research

6, Joliot Curie St., Dubna, Moscow Region, 141980, Russia

islamov@nf.jinr.ru

ORCID: 0000-0003-3837-0093

Kuklin Alexander I.

Joint Institute for Nuclear Research

6, Joliot Curie St., Dubna, Moscow Region, 141980, Russia

alexander.iv.kuklin@gmail.com

ORCID: 0000-0002-4530-2980

СВЕДЕНИЯ ОБ АВТОРАХ

УДОВЕНКО Станислав Александрович – младший научный сотрудник Высшей инженерно-физической школы Санкт-Петербургского политехнического университета Петра Великого.

195251, Россия, г. Санкт-Петербург, Политехническая ул., 29

udovenko_sa@spbstu.ru

ORCID: 0000-0002-0364-0797

НАБЕРЕЖНОВ Александр Алексеевич – доктор физико-математических наук, старший научный сотрудник Физико-технического института имени А. Ф. Иоффе РАН.

194021, Россия, г. Санкт-Петербург, Политехническая ул., 26

alex.nabereznov@mail.ioffe.ru

ORCID: 0000-0003-1929-032X

БОРИСОВ Сергей Аркадиевич – кандидат физико-математических наук, научный сотрудник Физико-технического института имени А. Ф. Иоффе РАН.

194021, Россия, г. Санкт-Петербург, Политехническая ул., 26

sergey.borisov@mail.ioffe.ru

ORCID: 0000-0002-7486-0391

СЫСОIEVA Анна Августовна – научный сотрудник Физико-технического института имени А. Ф. Иоффе РАН.

194021, Россия, г. Санкт-Петербург, Политехническая ул., 26

annasysoeva07@mail.ru

ORCID: 0000-0002-8876-9185



ТОМКОВИЧ Мария Вацлавовна – научный сотрудник Физико-технического института имени А. Ф. Иоффе РАН.

194021, Россия, г. Санкт-Петербург, Политехническая ул., 26
marya.tom83@gmail.com
ORCID: 0000-0002-1537-4107

ИСЛАМОВ Ахмед Хусаинович – кандидат физико-математических наук, старший научный сотрудник Объединенного института ядерных исследований.

141980, Россия, Московская область, г. Дубна, ул. Жолио Кюри, 6
islamov@nf.jinr.ru
ORCID: 0000-0003-3837-0093

КУКЛИН Александр Иванович – кандидат физико-математических наук, старший научный сотрудник Объединенного института ядерных исследований.

141980, Россия, Московская область, г. Дубна, ул. Жолио Кюри, 6
alexander.iv.kuklin@gmail.com
ORCID: 0000-0002-4530-2980

Received 08.10.2021. Approved after reviewing 08.10.2021. Accepted 18.10.2021.

*Статья поступила в редакцию 08.10.2021. Одобрена после рецензирования 08.10.2021.
Принята 18.10.2021.*